

THE PENNSYLVANIA STATE UNIVERSITY
SCHREYER HONORS COLLEGE

DEPARTMENT OF METEOROLOGY

GFS FORECAST SKILL FOR LONG-LIVED TROPICAL DISTURBANCES

ALICIA KLEES
Spring 2012

A thesis
submitted in partial fulfillment
of the requirements
for a baccalaureate degree
in Meteorology
with honors in Meteorology

Reviewed and approved* by the following:

Jenni Evans
Professor of Meteorology
Thesis Supervisor

Paul Markowski
Associate Professor of Meteorology
Honors Adviser

* Signatures are on file in the Schreyer Honors College.

ABSTRACT

Tropical cyclones are high-impact weather phenomena that numerical weather prediction models struggle to forecast. To improve the skill of a model in forecasting tropical cyclogenesis, the first step is to evaluate how the model forecasts long-lived tropical disturbances, as many of these may provide the incipient vortex for tropical cyclogenesis given favorable conditions. The skill of the Global Forecast System (GFS) model at forecasting tropical disturbances during August and September 2011 in the North Atlantic Ocean is examined in this project. Disturbances identified in GFS forecasts are verified using disturbances found in Wavetrak 850 hPa vorticity analyses. Vortex contingency tables are used to document the skill of GFS in capturing disturbances identified in the Wavetrak analyses and to document additional disturbances forecasted by GFS that were and were not observed in the Wavetrak analyses. Characteristics (major and minor axis lengths, size, vorticity, and eccentricity) of the disturbances identified in the Wavetrak analyses matched or unmatched with GFS forecasted disturbances are compared to identify the types of systems that GFS did and did not capture. Additionally, the vorticity and size of verified GFS forecasted disturbances are evaluated against the vorticity and size of the corresponding Wavetrak disturbances to determine the skill of GFS in forecasting those particular characteristics. While nearly 60% of GFS forecasts verify (are seen in Wavetrak), GFS only forecasted around 20% of the disturbances observed in Wavetrak analyses. Further, GFS does not have good skill in forecasting the vorticity of disturbances. Future work could compare the synoptic-scale environments for matched and unmatched disturbances to discern why GFS misses forecasting a plethora of observed disturbances.

TABLE OF CONTENTS

ACKNOWLEDGEMENTS.....iii

Chapter 1 Introduction1

Chapter 2 Methodology4

Chapter 3 Results & Discussion.....12

Chapter 4 Conclusions.....28

References.....30

ACKNOWLEDGEMENTS

I thank Dr. Jenni Evans for her immense guidance and support throughout this project. Without her direction and help, this project would not have been possible. I am also appreciative of the significant role she played in my maturation as both a scientist and a researcher. I am grateful to Tim Marchok for providing the GFS records and writing the code used to initially filter the GFS records. I am also grateful to Jason Dunion for creating the Wavetrak data sets. I thank Chris Velden for his assistance with acquiring data. I am also very appreciative of the encouragement and help throughout the project from Scott Sieron. Finally, I thank Dr. Paul Markowski for his helpful advice and support as my Honors Adviser for the past four years.

Chapter 1

Introduction

Tropical cyclones are high-impact weather phenomena in ocean basins. Tropical cyclones developing in the North Atlantic Ocean are of particular interest to the vulnerable populations in the islands of the Caribbean Sea and the eastern coasts of the United States, Mexico, and Central America. The vast destruction some tropical cyclones may cause as they approach land and make landfall underscores the need for accurate forecasting of these storms in all stages of their lifecycles. While accurately forecasting the track and timing of existing tropical cyclones approaching land is undoubtedly most relevant in terms of risk mitigation for potentially affected populations at short lead times, predicting the location and timing of the genesis of each cyclone is crucial as well. Knowing that there *will* be a storm is the first step in assessing the potential danger.

Numerical weather prediction models frequently struggle to forecast tropical cyclogenesis. To improve the current level of model forecast skill, evaluating past model performance is key. For example, Pratt and Evans (2009) examine GFS forecast skill during the 2002 and 2003 Atlantic hurricane seasons. They use Cyclone Phase Space (CPS; Hart 2003) analyses of GFS 6-hourly forecasts to determine which forecasts accurately predicted tropical cyclogenesis and which falsely forecasted tropical cyclogenesis. Also of interest are observed tropical cyclogenesis events the forecasts did not capture. Pratt and Evans (2009) find that less than a quarter of GFS forecasts successfully predicted tropical cyclogenesis events for some regions of the North Atlantic Ocean during these two hurricane seasons. False GFS forecasts of tropical cyclogenesis

made up over 70% of the total monthly genesis forecasts. Further, GFS forecasts did not capture twenty tropical lows (which could potentially evolve into tropical storms).

There are certainly many complex mechanisms involved in tropical cyclogenesis. Before diving in to further assess forecast skill, it is worth taking some time to consider what a successful genesis forecast must be able to capture. In the North Atlantic Ocean, tropical cyclones develop in association with tropical disturbances such as African easterly waves, subtropical storms, mesoscale convective systems, and equatorial Rossby waves (e.g., Landsea 1993; Davis and Bosart 2003; Simpson et al. 1993; Nitta and Takayabu 1985). However, very few of these disturbances actually develop into tropical cyclones; their development or lack thereof depends on conditions such as the amount of low-level relative vorticity and vertical wind shear (McBride and Zehr 1981). While a model must properly evolve the correct disturbances into tropical cyclones, equally crucial is that it successfully forecasts these disturbances in the first place. If a model cannot predict the existence and characteristics of these ‘candidate’ tropical disturbances with good skill, it cannot be expected to accurately forecast disturbances commencing tropical cyclogenesis.

The skill of the GFS model in forecasting North Atlantic tropical disturbances in August and September 2011 is examined here. All candidates for tropical cyclogenesis should be included in the set of convective systems examined. The characteristics of tropical systems occurring in Wavetrak satellite-derived vorticity analyses are documented. These characteristics are contrasted between systems that are and are not forecasted by GFS to determine and describe the types of disturbances GFS has skill in forecasting – and those it does not. Additionally, the characteristics of tropical

disturbances forecasted by GFS and the tropical disturbances in the analyses to which they verify are compared. The goal is to determine not only the skill of GFS in forecasting systems, but also to gain insight on why GFS misses forecasting some systems and how that issue can be improved.

Chapter 2

Methods

To evaluate the skill of the GFS model in forecasting tropical disturbances, we examine Wavetrak satellite-derived vorticity analyses, document the characteristics of systems identified and compare their distributions in space and time with similar systems diagnosed in GFS. The data and methodology used are described in this chapter.

a. Time period and region of interest

Tropical disturbances from August and September 2011 are examined. These two months typically have high levels of tropical activity, and August and September 2011 were no exception, with twelve named storms, six of them achieving hurricane strength (NHC 2012). The domain of interest for this project is 5°N - 25°N , 15°W - 85°W , which is where the majority of North Atlantic tropical cyclogenesis occurs in August and September. This is seen, for example, in Fig. 1, the tropical cyclogenesis location climatology for the first week of September.

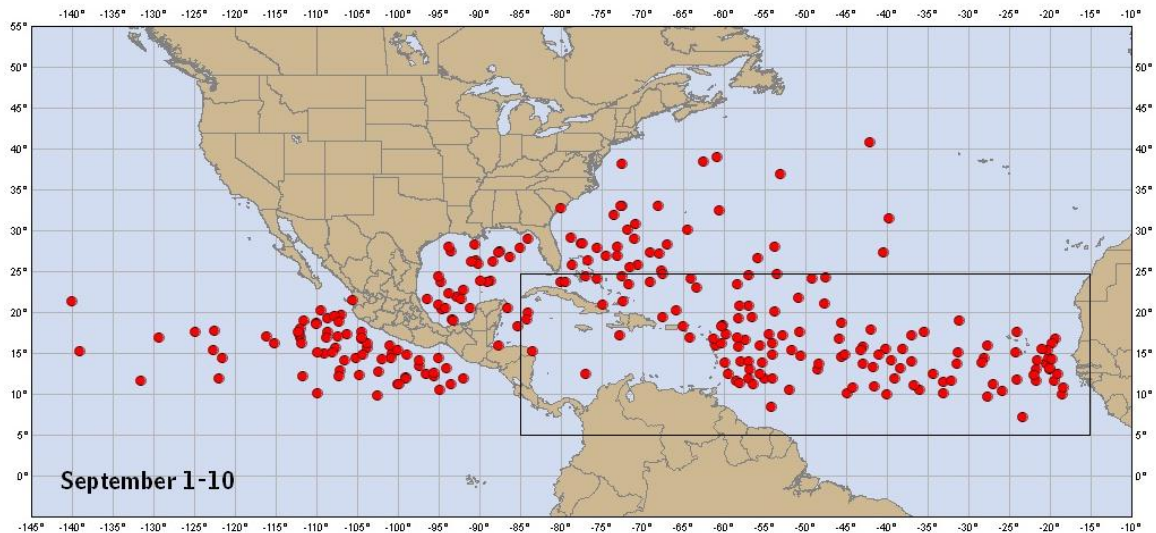


FIG 1. Tropical cyclogenesis location climatology, 1851-2009. The rectangle denotes the region of interest for this project. Image courtesy of the National Hurricane Center at http://www.nhc.noaa.gov/climo/images/9_1_10_nhc.png.

b. Wavetrak data overview

The observational database for this study is the Wavetrak 850 hPa relative vorticity analyses; Wavetrak data are produced by the Cooperative Institute for Meteorological Satellite Studies at the University of Wisconsin. The database is created by using NOGAPS model data as a first guess background field, deriving cloud-drift winds from satellite data, and employing a recursive filtering technique (CIMSS/University of Wisconsin 2012). The domain for the Wavetrak data (0°N - 35°N , 0°W - 100°W)¹ has a grid spacing of $\sim 0.0839^{\circ}$ in the east-west direction and $\sim 0.0897^{\circ}$ in the north-south direction (about $9.32 \text{ km} \times 9.97 \text{ km}$ spacing). Three-hourly Wavetrak data from 0Z on August 1, 2011 to 18Z on September 30, 2011 are used.

c. Identification of tropical disturbances in Wavetrak analyses

Candidate tropical disturbances are identified in the Wavetrak data using image processing concepts and algorithms. A distinct system is defined by all gridpoints connected via corners or edges with values of 850 hPa relative vorticity exceeding a threshold of $20 \times 10^{-6} \text{ s}^{-1}$. An elliptical representation (with the same normalized second central moment as the system) is assumed for the purpose of gaining information on the system size (major and minor axis). This is a reasonable assumption to make, as the majority of systems appear to be fairly elliptical in shape. Only systems with elliptical equivalent major and minor axes both exceeding 0.5° are retained for further analysis. This filters out any areas of vorticity above the threshold, but too small to represent candidate tropical disturbances.

¹Recall that the study domain is (5°N - 25°N , 15°W - 85°W).

d. Identification of tropical disturbances in GFS forecasts

The GFS 6 hourly forecasts are produced at 27 km horizontal resolution (NCEP EMC 2011). Tropical disturbances are found in the forecasts using the Geophysical Fluid Dynamics Laboratory vortex tracker (Marchok 2010). According to Marchok (2010), the tracker uses the primary parameters of 10 m relative vorticity, 700 hPa relative vorticity, 850 hPa relative vorticity, mean sea level pressure, 700 hPa geopotential height, and 850 hPa geopotential height. A Barnes analysis is conducted on these parameters to find the minimum or maximum of each, and all ensuing positions are combined to find and track a vortex (Marchok 2010). Records of all vortices found in forecasts from each model cycle are produced (Marchok 2010). For the purposes of this project, only systems with centers within the domain of 5°N-25°N, 15°W-85°W which persist for at least five consecutive forecasts (twenty-four hours) in a given forecast cycle are considered. Areas of convection that cannot maintain themselves for at least twenty-four hours are not considered to be candidate tropical disturbances.

e. Verification of GFS forecasts

To verify the systems forecasted by GFS against the systems in the Wavetrak analyses, an algorithm is applied for each specific forecast of a system. All Wavetrak systems existing at the forecast validation time are examined. If the center of the forecasted system falls anywhere within a Wavetrak system (and it can only be found within one, since the Wavetrak systems are all distinct), then the forecasted system has been verified. See Fig. 2 for a visualization of this scenario.

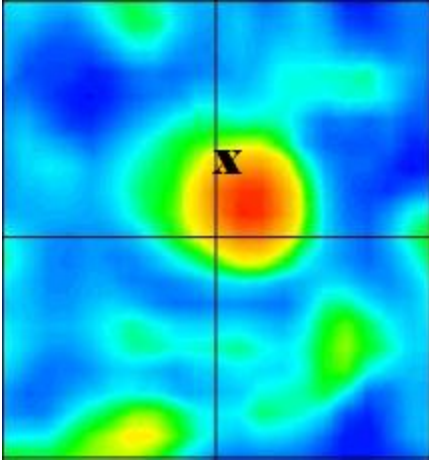


FIG 2. A successful GFS forecast. The 'X' denotes the center of the system forecasted by GFS. It easily falls within the bounds of the analysis system, defined by the transition from the yellow to green. Original Wavetrak image courtesy of University of Wisconsin --CIMSS. Similar products can be found at <http://tropic.ssec.wisc.edu/archive/>.

On the other hand, if there is no match between the forecasted system and any of the Wavetrak systems for the validation time, then the forecasted system does not verify. Refer to Fig. 3 for a representation of this scenario in its most extreme case.

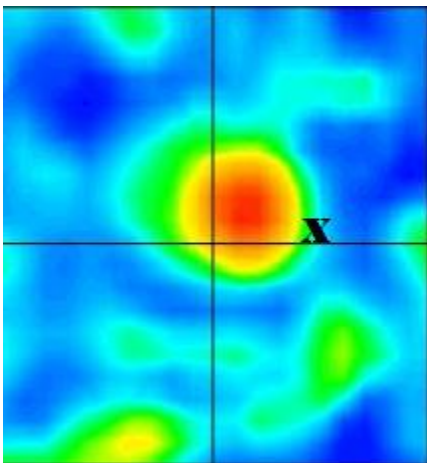


FIG 3. Like Fig. 2, except that now the GFS forecasted system does not fall within the bounds of any system identified in the Wavetrak analysis, although it comes very close. Original Wavetrak image courtesy of University of Wisconsin -- CIMSS.

Systems identified in the Wavetrak analyses and forecasted by GFS are referred to as “matched,” while the remaining Wavetrak systems are designated as “unmatched.” Unless stated otherwise, the category of matched systems can contain a particular system multiple times, since GFS forecasts from different model forecast cycles having the same validation time can verify with the same Wavetrak system multiple times.

f. System characteristics

System characteristics are retrieved and calculated for verified forecasted systems and both matched and unmatched Wavetrak analysis systems. These characteristics are summarized in Table 1. Note that the radius of GFS forecasted systems is defined using the radius of the outer closed isobar (ROCI), rather than the vorticity threshold used to find the axis lengths of the Wavetrak systems.

GFS Verified Forecasted Systems			
System Characteristic	Description	Represents	Calculation
850 hPa relative vorticity	Maximum relative vorticity found near 850 hPa center	System intensity	Retrieved from forecast
Radius (r)	Mean radius of last closed isobar	System extent	Retrieved from forecast
Size	Area of circle	System extent	πr^2
Matched and Unmatched Wavetrak Analysis Systems			
System Characteristic	Description	Represents	Calculation
850 hPa relative vorticity	Maximum 850 hPa relative vorticity in system	System intensity	Retrieved from analysis
Major axis (a)	Length of major axis of equivalent ellipse	System extent	Retrieved through elliptical assumption made on analysis
Minor axis (b)	Length of minor axis of equivalent ellipse	System extent	Retrieved through elliptical assumption made on analysis
Size	Area of equivalent ellipse	System extent	$\frac{1}{4}\pi ab$
Eccentricity	Ratio of length of minor axis to length of major axis	System organization	b/a

TABLE 1. Description of system characteristics.

g. Data issues

Three issues are found in the Wavetrak analysis data; they are handled in the following ways. First, there are no 6Z Wavetrak data available for thirty-two days during the GOES eclipse season (Jason Dunion 2012, personal communication). While 3Z and 9Z Wavetrak data for those days do exist, the GFS forecast locations are only available every six hours (0Z, 6Z, 12Z, 18Z). Verifying 6Z forecasts using Wavetrak analysis systems from 3Z or 9Z is not equivalent to using Wavetrak analysis systems from 6Z. Therefore, to maintain consistency, all GFS forecasts with a validation time corresponding to a date with missing 6Z data are disregarded.

Second, the domain for Wavetrak analyses is greater in extent than the domain of interest for the GFS forecasts. System identification in the Wavetrak analyses is allowed to take place beyond the domain for the GFS forecasted systems (5°N - 25°N , 15°W - 85°W) so the characteristics of any system that straddles a boundary of the GFS domain can be calculated properly. However, a GFS forecasted system center has less of a chance of falling within a Wavetrak system that is partially located outside the domain compared to a Wavetrak system that is fully contained within the domain. Fig. 4 shows an example of a Wavetrak system partially located outside of the domain.

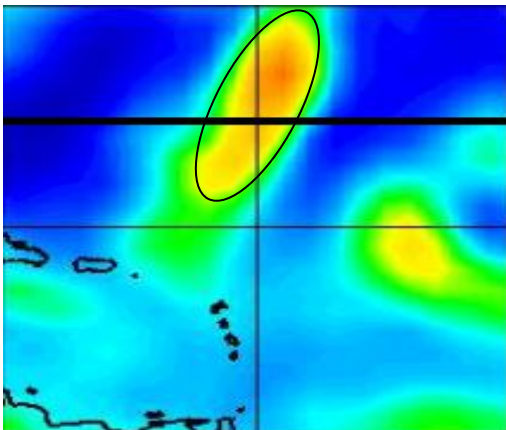


FIG 4. An analysis system partially located outside of the domain for the GFS forecasted systems. The thick latitude line indicates the northern edge of the domain, 25°N . Original Wavetrak image courtesy of University of Wisconsin --CIMSS.

Thus, any systems in Wavetrak with geometric centers outside of the GFS domain are excluded from any of the results presented here.

Finally, when a system is named by the National Hurricane Center as either a tropical depression, tropical storm, or hurricane, a bogus vortex is inserted into the Wavetrak first-guess field at the given analysis time (with occasionally a temporal offset from when the National Hurricane Center declared the status of the storm, due to the real-time nature of the Wavetrak products). The system designated with the cyclone symbol in Fig. 5 is an example of a bogussed vortex in the Wavetrak analyses.

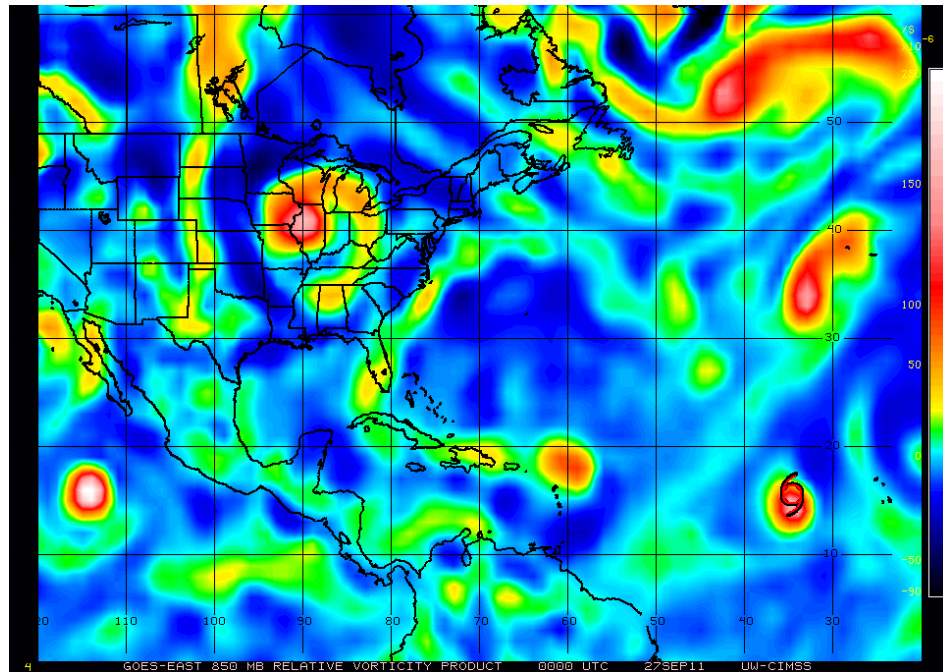


FIG 5. An example of how a bogussed vortex is denoted. This particular bogussed vortex is Tropical Storm Phillippe. Wavetrak image courtesy of University of Wisconsin --CIMSS.

Vortex bogussing is used for each Wavetrak analysis time for any system that is tropical depression strength or stronger. If the system dips below tropical depression strength, subsequent analysis times are not affected by the prior vortex bogussing.

The bogussed vortex is given predetermined characteristics such as size and 850 hPa relative vorticity, so it is impossible to meaningfully analyze the characteristics of any systems consisting of a bogussed vortex. Thus, these systems must be disregarded when comparing their respective characteristics to the forecasted systems. However, given that these systems are much stronger than typical tropical convective systems, we continue to evaluate the ability of GFS to forecast them. It should be noted that no bogus vortex is used in the GFS model.

Results and discussion are presented in the next chapter.

Chapter 3

Results and Discussion

The number and characteristics of Wavetrak analysis systems forecasted and not forecasted by GFS, and systems forecasted by GFS that did and did not verify with Wavetrak analysis systems, are analyzed and these diagnostics are presented here.

a. Vortex contingency tables

Vortex contingency tables (Tables 2 and 3) are employed to summarize the skill of the GFS model in forecasting tropical disturbances. First, we consider systems forecasted by GFS which verified with Wavetrak analyses and those that did not (Table 2). When including verification with systems that are bogussed in the Wavetrak analyses, nearly 60% of GFS forecasts verified. Systems observed in the Wavetrak analyses were almost always evident in the GFS analyses (zero hour lead time) (Table 2). The percent of forecasts verified decreases with increasing lead time, but the forecast skill does not decrease significantly until a 120 hour lead time (Table 2). It is not surprising that at 180 hour lead time, GFS correctly forecasts about only 1 out of 5 systems (Table 2). The vortex contingency table that does not include bogussed systems shows that even just with these remaining ‘weak’ systems, GFS is still successfully forecasting more systems than it is falsely forecasting at lead times up to 48 hours.

Number of forecasts							
GFS Forecast Lead Time	All	0 hour	24 hour	48 hour	72 hour	120 hour	180 hour
Verified with Wavetrak analysis (including bogussed systems)	3584	174	205	188	137	71	26
Did not verify with Wavetrak analysis	2558	3	12	41	86	125	111
Percent of forecasts							
GFS Forecast Lead Time	All	0 hour	24 hour	48 hour	72 hour	120 hour	180 hour
Verified with Wavetrak analysis (including bogussed systems)	58.4	98.3	94.5	82.1	61.4	36.2	19.0
Did not verify with Wavetrak analysis	41.6	1.7	5.5	17.9	38.6	63.8	81.0
Number of forecasts							
GFS Forecast Lead Time	All	0 hour	24 hour	48 hour	72 hour	120 hour	180 hour
Verified with Wavetrak analysis (excluding bogussed systems)	1735	68	85	96	72	41	13
Did not verify with Wavetrak analysis	2558	3	12	41	86	125	111

TABLE 2. Vortex contingency table for GFS forecasts.

GFS fails to forecast (even when including the GFS analyses, 0 hour lead time) almost 80% (1285/1632) of the systems detected in the Wavetrak analyses (Table 3). However, when GFS does forecast a system, it is forecasted persistently across model runs. This is evidenced by the number of verifications being nearly ten times greater than the number of unique Wavetrak analysis systems forecasted by GFS; sometimes, there are multiple forecasts (with varying lead times) of a system with the same validation time which all match with the same system in the analysis. When bogussed systems are not considered, the total number of verifications (including repeats) decreases significantly

(Table 3), as GFS is more persistent with forecasts of stronger systems between model runs (Section 3e).

Wavetrak systems (including bogussed):	Number of systems
Not forecasted by GFS	1285
Forecasted by GFS (no repeats)	347
Wavetrak systems (including bogussed):	Number of systems
Not forecasted by GFS	1285
Forecasted by GFS (including repeats)	3584
Wavetrak systems (not including bogussed):	Number of systems
Not forecasted by GFS	1281
Forecasted by GFS (including repeats)	1735

TABLE 3. Vortex contingency table for Wavetrak analysis systems.

The GFS forecast skill documented in this last vortex contingency table (Table 3) raises the question of why GFS is able to forecast some systems well, but misses many well observed systems entirely. A comparison of the characteristics of the matched and unmatched systems in the Wavetrak analyses will help answer this question.

b. Major and minor axes

The Wavetrak system identification methodology assumed ellipticity of systems. Thus, all systems identified possess major and minor axes. These axes describe the size and shape of a system. The distribution of major axis length for all non-bogussed systems is analyzed in Fig. 6. (All further plots exclude bogussed systems as well.)

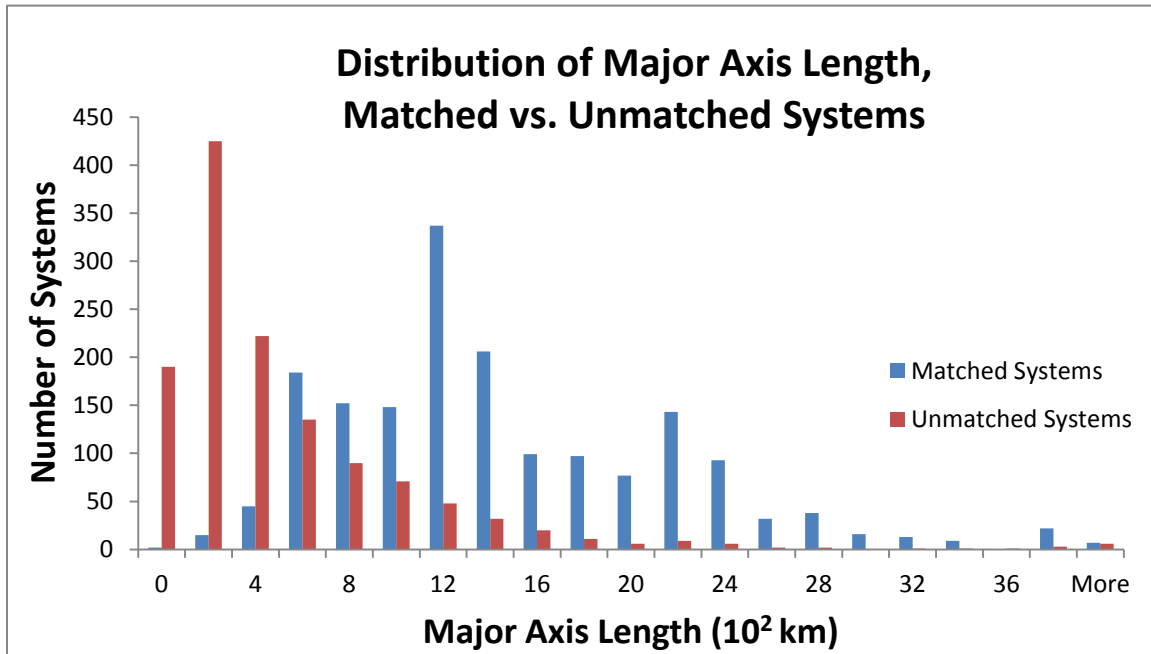


FIG 6. Distribution of major axis length for matched (blue) vs. unmatched (red) Wavetrak analysis systems.

It is evident that the length of the major axis of matched systems is distributed more widely and tends to be greater than the length of the major axis of unmatched systems. The distribution for matched systems has three peaks, and the highest of the three is the 1200 km bin. The peak for unmatched systems is only the 200 km bin. Interestingly, in both matched and unmatched systems (though predominantly matched systems), there are major axis lengths exceeding 3000 km. This is clearly too large of a scale to be associated with the more prevalent tropical disturbances such as individual mesoscale convective systems.

For example, Fig. 7 shows a matched system with a major axis length of around 4100 km. This system is likely a disorganized cluster of thunderstorms associated with the ITCZ (not a cluster of MCSs because the system does not strengthen or weaken with

the diurnal cycle; rather, it just dissipates within a day).

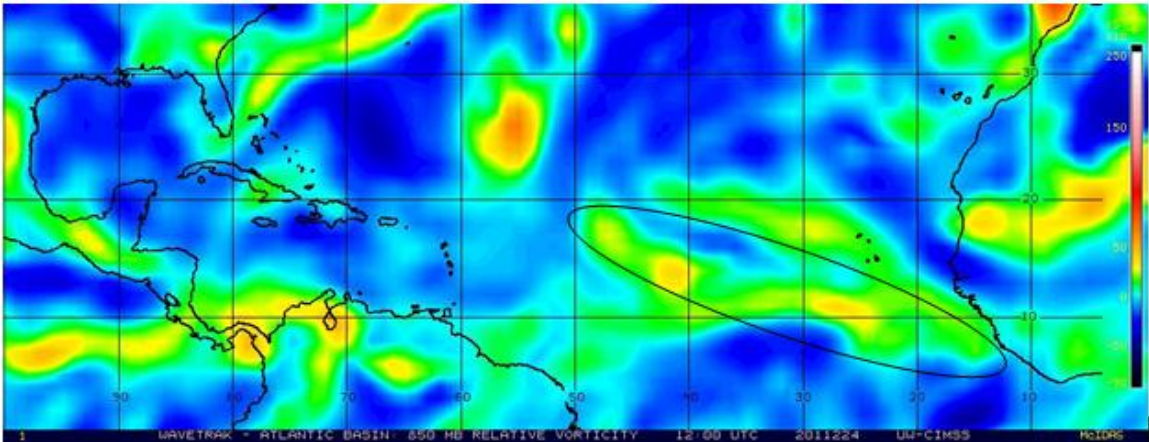


FIG 7. Wavetrak 850 hPa relative vorticity plot from 12 Z on August 12, 2011. Image courtesy of University of Wisconsin --CIMSS.

On the opposite end of the major axis length spectrum is the example noted in Fig. 8.

Given the size and vorticity signature, it may be an evolving mesoscale convective system or subtropical storm.

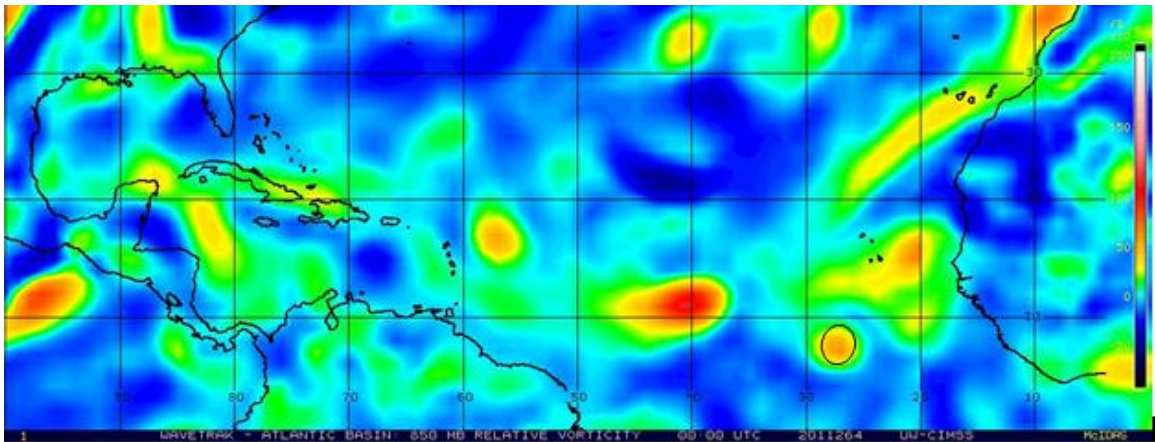


FIG 8. Wavetrak 850 hPa relative vorticity plot from 0Z on September 21, 2011. Image courtesy of University of Wisconsin --CIMSS.

There are examples of unmatched systems with large major axes as well. The system in Fig. 9 has a long major axis, but GFS does not forecast the center of any system to fall within this system. The system is a cluster of mesoscale convective systems

embedded in the ITCZ (evidenced by their apparent weakening and strengthening with the diurnal cycle).

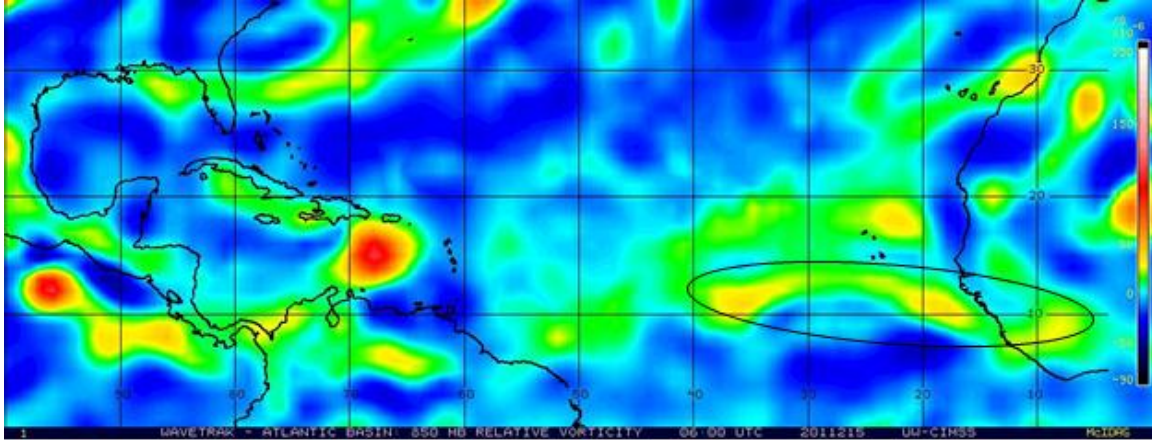


FIG 9. Wavetrak 850 hPa relative vorticity plot from 6Z on August 3, 2011. Image courtesy of University of Wisconsin --CIMSS.

The distribution of minor axis length peaks at smaller values than does the distribution of major axis length and has a much smaller range, as displayed in Fig. 10.

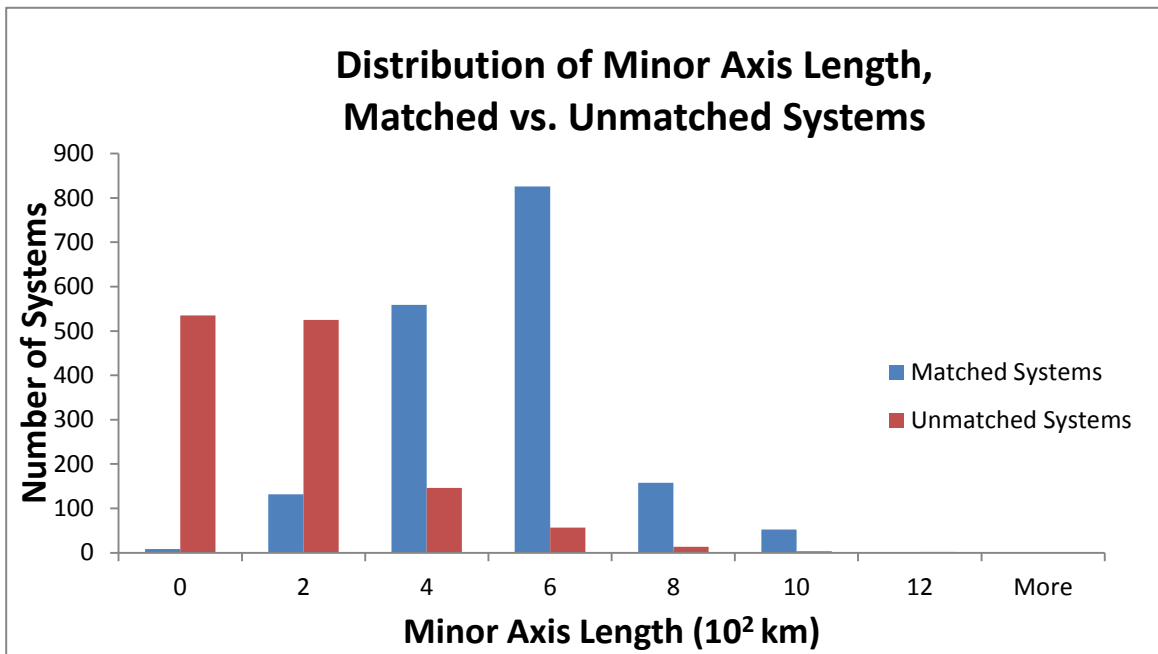


FIG 10. Distribution of minor axis length for matched (blue) vs. unmatched (red) Wavetrak analysis systems.

As seen in the major axis length distribution, unmatched systems typically have shorter axis lengths than matched: almost 85% (1060/1281) of minor axis lengths of the unmatched systems fall below 400 km, while fewer than 10% (140/1735) of the matched systems are this small. The minor axis lengths for matched systems peak around the 600 km bin and those for unmatched systems peak between 0-200 km.

The matched versus unmatched major and minor axis length distributions are reasonable: to the first-order, systems that have a larger major (minor) axis length are more likely to be of a larger size and therefore have a greater possible area into which a GFS forecasted system center can fall than systems with smaller axis lengths. However, major and minor axis lengths are not always the best proxy for system size; for example, a system with a long major axis but a very short minor axis may cover an area equal to or less than a system with a medium major axis and a medium minor axis.

c. Size

Given the potential issue with using major and minor axes as a proxy for size all of the time, size as defined by area of the system is another good characteristic to consider. Fig. 11 displays the distribution of size for matched and unmatched systems.

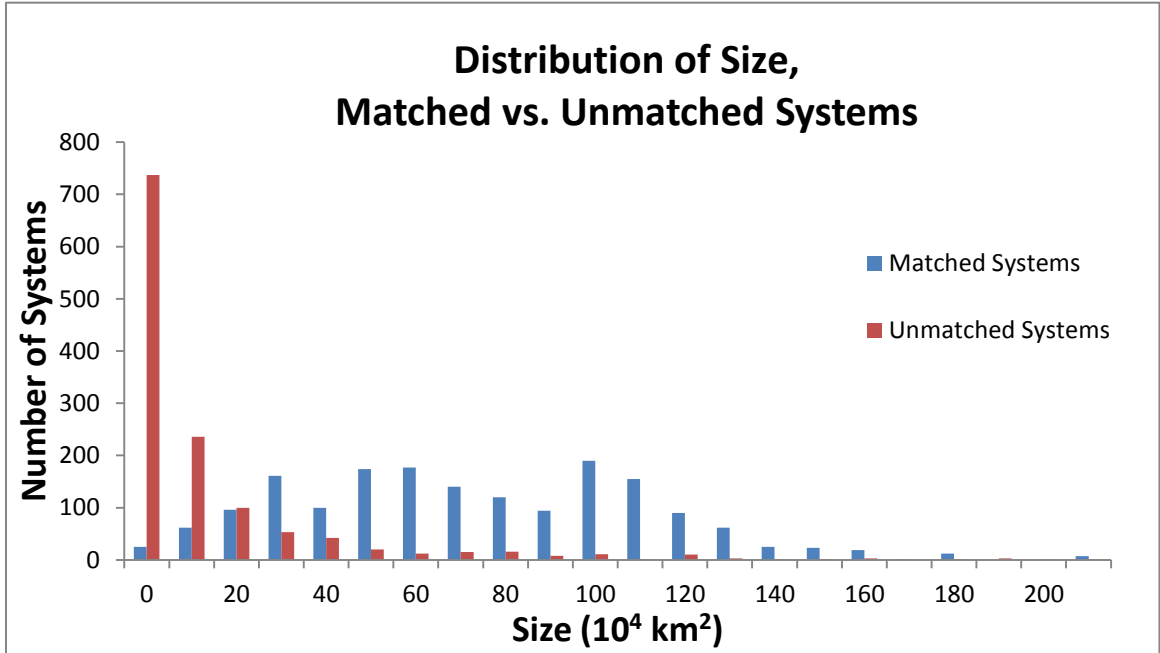


FIG 11. Distribution of size, defined by area, of matched (blue) vs. unmatched (red) Wavetrak analysis systems.

As initially suggested by the comparison of axis lengths, unmatched systems are typically smaller than matched systems. In fact, the vast majority (around 75%) of unmatched systems are less than $20 \times 10^4 \text{ km}^2$ in size and there are very few in the higher end of the size spectrum. Matched systems have a fairly even size distribution between about $10 \times 10^4 \text{ km}^2$ and $130 \times 10^4 \text{ km}^2$.

For a sense of how forecasted system size compares to size of the analysis system matching the forecasted system, refer to Fig. 12.

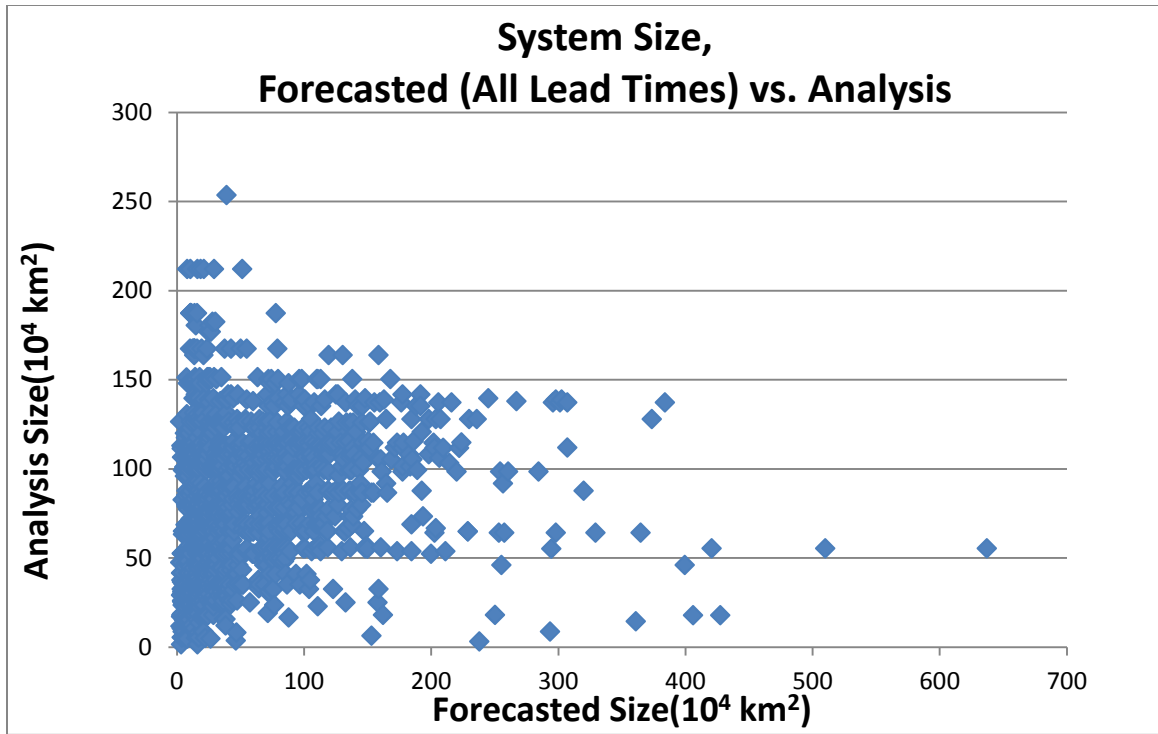


FIG 12. Size of the systems forecasted by GFS versus the size of the corresponding matched systems in the analysis.

Over 75% of the time, GFS under-forecasts the system size. Many of the differences in system sizes between analysis and forecasts likely derive from the differences in the methodologies of identifying systems and determining size. In the Wavetrak analyses, multiple centers of vorticity connected by small threads of vorticity (a feature seen frequently in the region of the ITCZ) are identified to be one contiguous, large system, rather than several smaller distinct systems. GFS is more apt to forecast a distinct system within this larger feature, rather than the larger feature itself. Fig. 13 illustrates an example of this. Note that the black dot indicates the center of the GFS forecasted system, the circle the extent of the GFS forecasted system based on the given radius of the outermost isobar, and the oval the approximate elliptical representation of the system in Wavetrak to which this forecasted system was matched.

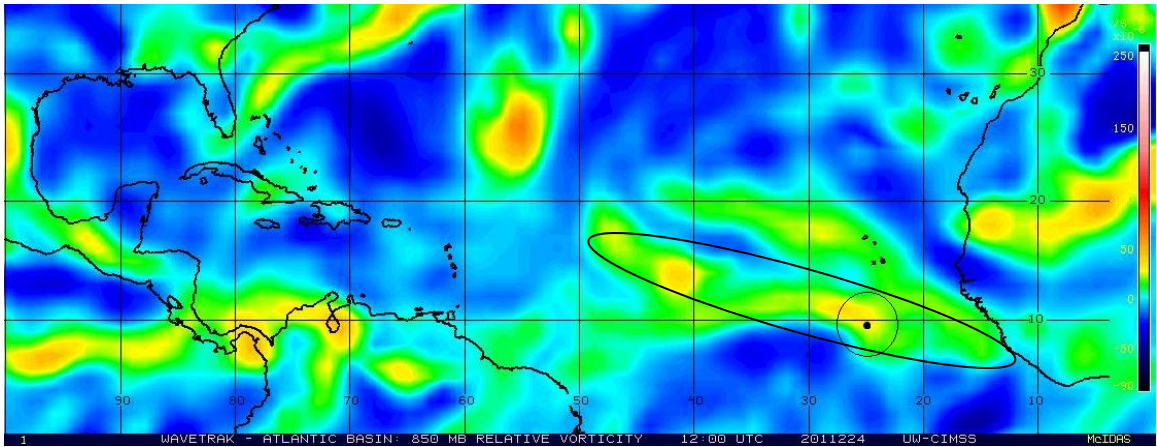


FIG 13. Wavetrak 850 hPa relative vorticity plot from 12Z on August 12, 2011. Image courtesy of University of Wisconsin --CIMSS.

Clearly, the size of the two systems shown in Fig. 13 can't be fairly compared.

On a related note, using the radius of the outermost closed isobar of the system to define size for GFS forecasted systems versus using the equivalent elliptical representation of the area of vorticity to define size for Wavetrak analysis systems may give different sizes based on geometry, as well as due to the differences from using system extent dictated by pressure patterns versus vorticity patterns. Therefore, while it is reasonable to compare the size of matched and unmatched systems within the Wavetrak analyses, the size of Wavetrak analysis systems cannot meaningfully be compared to the size of forecasted systems.

d. Eccentricity

System shape, eccentricity, is another interesting characteristic to examine. A circular system will have an eccentricity of one, while smaller eccentricity values correspond to a system with a more elongated or elliptical shape. Refer to Fig. 14 for the distribution of eccentricity.

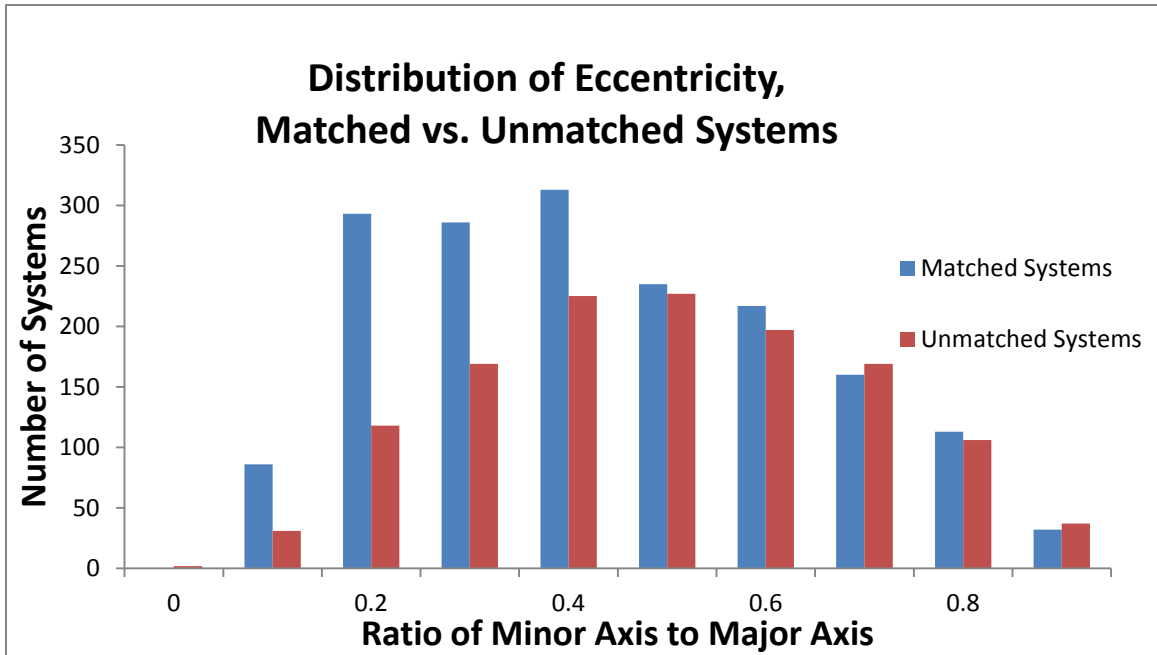


FIG 14. Distribution of eccentricity for matched (blue) vs. unmatched (red) Wavetrak analysis systems.

Unmatched systems have an approximate normal distribution of eccentricity centered on the 0.4 and 0.5 bins (Fig. 14). There certainly seems to be a tendency for matched systems to have more elliptical shapes. In fact, a little over 55% of matched systems have an eccentricity below 0.5, while only around 40% of unmatched systems fall in this category. This is likely the case because, as displayed in Fig. 15, larger systems tend to have lower eccentricities than smaller systems, and, as concluded in the previous section, matched systems tend to be larger in size.

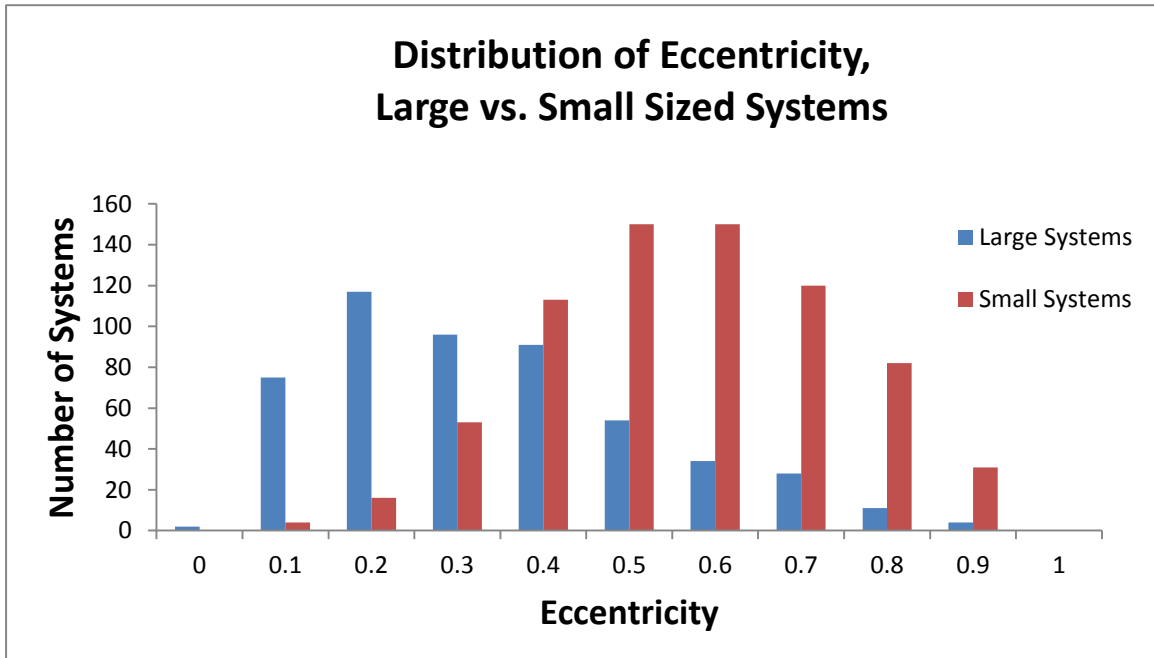


FIG 15. Distribution of eccentricity for “large” systems (sizes greater than $140 \times 10^4 \text{ km}^2$, blue) and “small” systems (sizes less than $9 \times 10^4 \text{ km}^2$, red).

Fig. 16 shows one such example of a matched, large system (major axis spanning over 3400 km) with low eccentricity.

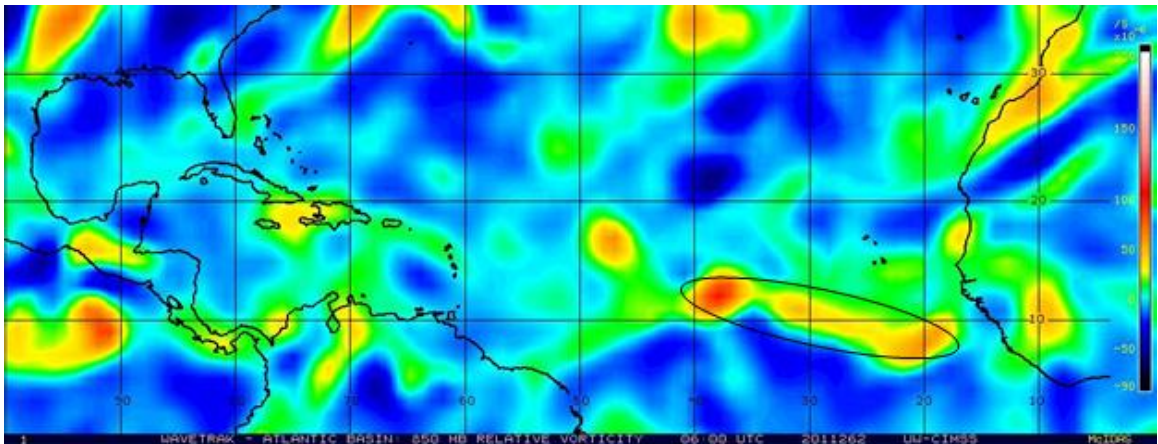


FIG 16. Wavetrak 850 mb relative vorticity plot from 6Z on September 19, 2011. Image courtesy of University of Wisconsin --CIMSS.

On the opposite end of the spectrum, the system highlighted in Fig. 8 has an eccentricity very close to one and a very short major axis length. On its own, then, eccentricity does not seem to be a good discriminator between matched and unmatched systems, given the

apparent strong impact of system size on eccentricity and the tendency for smaller storms to be unmatched and vice versa.

e. Vorticity

Finally, to complete the picture, the characteristic of system vorticity, as a representation of system intensity, is investigated (Fig. 17).

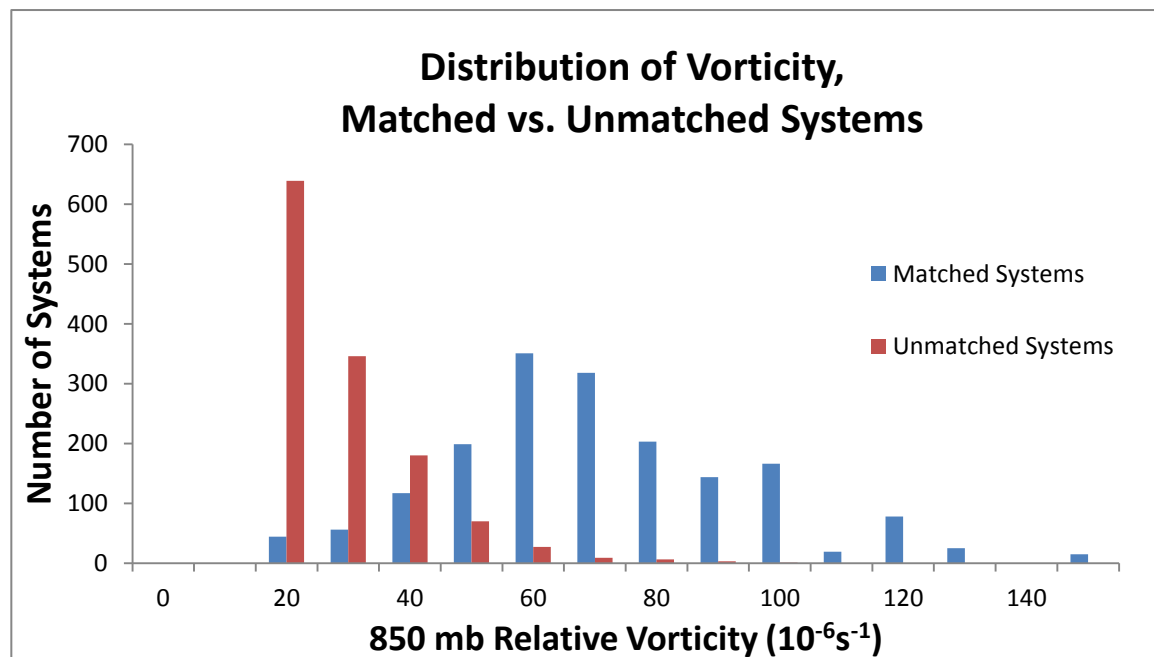


FIG 17. Distribution of vorticity for matched (blue) vs. unmatched (red) Wavetrak analysis systems.

The vorticity of matched systems is distributed approximately normally, though slightly skewed to the right, with the $60 \times 10^{-6} \text{ s}^{-1}$ bin as the mean and mode of the distribution. The distribution of the vorticity for unmatched systems is strongly skewed to the left of this distribution, with over 95% of the unmatched systems falling below the mean bin for the matched systems. Recalling that the minimum vorticity of a system identified was constrained to be at least $20 \times 10^{-6} \text{ s}^{-1}$, it appears that GFS has a tendency to under-forecast weaker systems, as would be expected.

The vorticity distribution for matched systems split up by varying lead times (Fig. 18) suggests that there isn't a strong relationship between the intensity of analysis systems that GFS forecasts and the lead time of the forecasts.

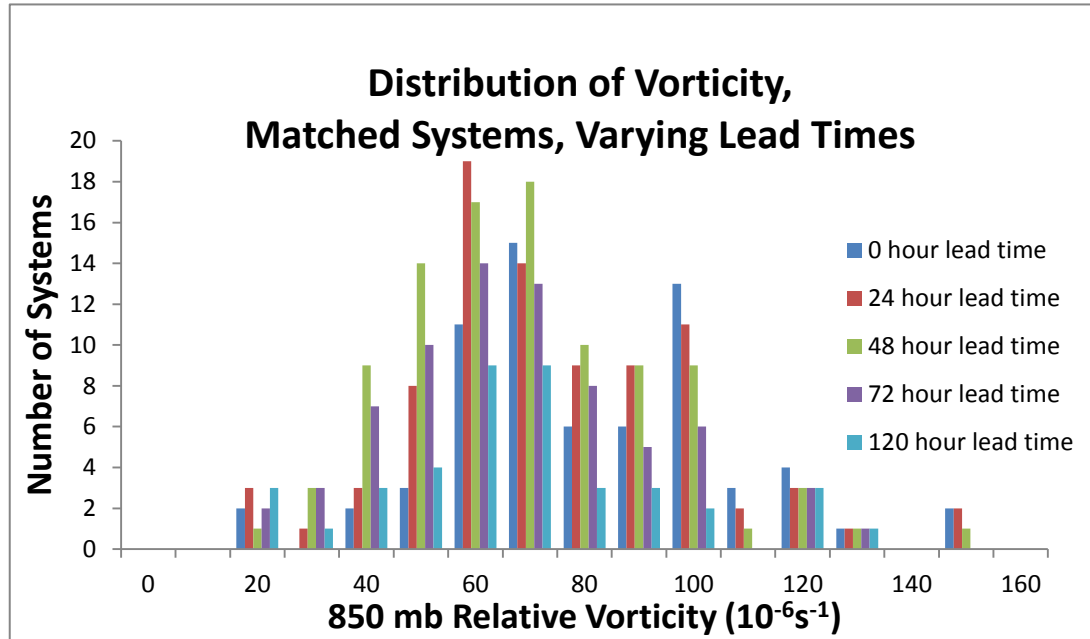


FIG 18. Distribution of vorticity of matched Wavetrak analysis systems for various lead times.

The shapes of the vorticity distributions for all lead times are comparable and cover similar ranges of vorticity. Surprisingly, Wavetrak analysis systems matching with GFS forecasted systems at 120 hour lead time have a fairly even vorticity distribution and peak at moderate vorticity values. One might expect that the Wavetrak analysis systems matched at later lead times would be more intense, since GFS better captures their existence far in advance. Further insight can be acquired through analyzing how GFS performs in forecasting system intensity and with what skill, especially for large lead times. This is done by examining the differences between forecasted system vorticity and matched analysis system vorticity, as seen in Fig. 19.

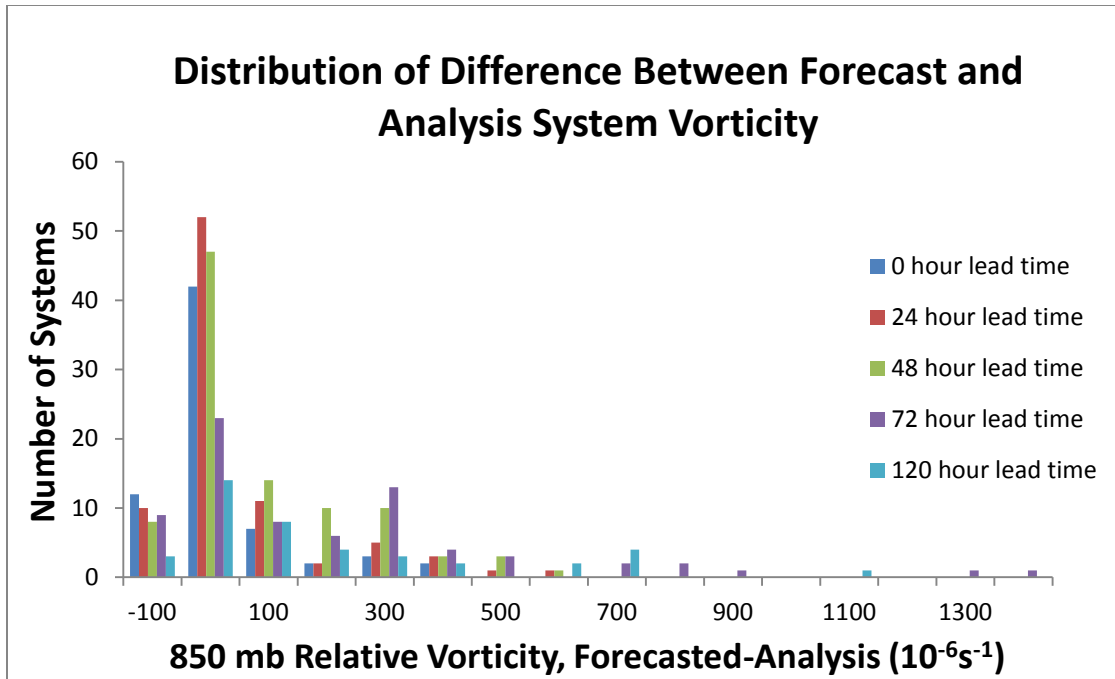


FIG 19. Distribution of the difference between vorticity of GFS forecasted systems and vorticity of Wavetrak analysis systems for various lead times.

At all lead times analyzed, GFS frequently over-forecasts the vorticity. This is especially the case with systems forecasted at 72 hour or 120 hour lead times, with some differences exceeding $700 \times 10^{-6} \text{s}^{-1}$. As all analysis systems have vorticity below $160 \times 10^{-6} \text{s}^{-1}$, this means that GFS sometimes over-forecasts vorticity and therefore system intensity by over an order of magnitude! GFS performs slightly better in capturing intensity at the analysis time (0 hour lead time) than at other lead times, evidenced by the left skew of the zero hour distribution (navy blue). However, at analysis time, GFS would be expected to have even more skill in forecasting system intensity than demonstrated here, given that current observations are used in the analysis and so to initialize model runs.

One possible explanation for the significant over-forecasting of system intensity in GFS forecasts with 72 and 120 hour lead time is that GFS might be forecasting

systems of tropical depression strength or higher to develop (earlier than they actually do in Wavetrak analyses, because otherwise the GFS forecasts would be matching bogussed systems in the Wavetrak analyses and would therefore be excluded from all examination of systems characteristics). However, in only three 72 hour forecasts and no 120 hour forecasts of system vorticity exceeding $160 \times 10^{-6} \text{ s}^{-1}$ does GFS declare the system to be of tropical depression strength or higher! It is therefore unclear what types of systems GFS is forecasting to have such high intensities.

Vorticity, as a measure of intensity, can be used to distinguish between matched and unmatched systems with reasonable success – matched systems tend to be more intense and unmatched systems less so – but GFS doesn't have strong skill in forecasting system intensity.

A summary of these results, with suggestions for future research, follow in the next chapter.

Chapter 4

Conclusions

In this project, we examined the number and characteristics of systems observed in Wavetrak analyses that were and were not forecasted by GFS and systems forecasted by GFS that did and did not verify with Wavetrak analysis systems to describe the types of disturbances GFS has skill in forecasting – and those it does not.

We find that 60% of systems forecasted by GFS verify. Forecast skill is above 50% for forecasts analyzed up to 72 hour lead time. Approximately 20% of the systems observed in the Wavetrak analyses are forecasted by GFS, but when a system does appear in the model, GFS tends to forecast the system persistently across model runs.

Physical characteristics, vorticity, size, and major and minor axis lengths, of systems forecasted by GFS and observed in Wavetrak analyses differ (in physically meaningful ways) from systems that are not forecasted by GFS. As would be expected, GFS forecasts have a tendency to catch stronger, larger systems than weaker, smaller systems. The size and vorticity characteristics are therefore optimal in predicting the types of systems that are most likely to be forecasted by GFS. Because of its strong dependence on the geometric assumptions used to identify Wavetrak systems and on the system size, eccentricity cannot be used to distinguish between these two types of systems in a physically meaningful way.

The skill of GFS in forecasting the maximum vorticity of a system is poor. GFS frequently over-forecasts the intensity of a system, sometimes by over an order of magnitude. The skill of GFS in forecasting the system size cannot be evaluated due to the significant difference in the definition of size for systems forecasted by GFS (outer

closed isobar of surfaced pressure) versus systems in the Wavetrak analyses (relative vorticity threshold).

Using the insight gained in this project of classes of systems forecasted and not forecasted by GFS, future research should examine the 80% of systems in the Wavetrak analyses which GFS does not forecast. One interesting approach would be to investigate synoptic-scale features potentially affecting the systems of interest and the ability of GFS to forecast them. A larger region than the domain analyzed here should be used to capture interactions among a range of synoptic systems. If GFS missed forecasting a number of smaller systems, was it because it did not capture the monsoon trough in which they were embedded adequately? Once such questions are answered, the next step would be to verify how well GFS performed in forecasting tropical cyclogenesis during August and September 2011 and the factors that play a role in its performance. Ultimately, conclusions formed from such research could be applied to design future upgrades to the GFS model.

References

- CIMSS/University of Wisconsin, cited 2012: Tropical Cyclones -- Wavetrak. [Available online at <http://tropic.ssec.wisc.edu/misc/wavetrak/info.html>].
- Davis, C.A. and L.F. Bosart, 2003: Baroclinically Induced Tropical Cyclogenesis. *Mon. Wea. Rev.*, **131**, 2730–2747.
- Hart, R., 2003: A cyclone phase space derived from thermal wind and thermal asymmetry. *Mon. Wea. Rev.*, **131**, 585-616.
- Landsea, C.W., 1993: A climatology of intense (or major) Atlantic hurricanes. *Mon. Wea. Rev.*, **121**, 1703-1713.
- Marchok, T., 2010: Use of the GFDL Vortex Tracker. Geophysical Fluid Dynamics Laboratory, 13 pp.
- McBride, J. L. and R. Zehr, 1981: Observational analyses of tropical cyclone formation: II. Comparison of non-developing versus developing systems. *J. Atmos. Sci.*, **38**, 1132-1151.
- NCEP EMC, cited 2012: Global Forecast System – Implementations. [Available online at <http://www.emc.ncep.noaa.gov/GFS/impl.php>].
- NHC, cited 2012: 2011 Atlantic Hurricane Season. [Available online at <http://www.nhc.noaa.gov/2011atlan.shtml>].
- Nitta, T., and Y. Takayabu, 1985: Global analysis of the lower tropospheric disturbances in the Tropics during the northern summer of the FGGE year. Part II: Regional characteristics of the disturbances. *Pure Appl. Geophys.*, **123**, 272–292
- Pratt, A., and J. L. Evans, 2009: Evaluation of operational model forecast skill for Atlantic tropical cyclones. *Weather and Forecasting*, **24**, 420-435.

Simpson, J., E. Ritchie, G. J. Holland, J. Halverson, and S. Stewart, 1997: Mesoscale interactions in tropical cyclone genesis. *Mon. Wea. Rev.*, **125**, 2643–2661.

Academic Vita

Alicia M. Klees

EDUCATION:

B.S. Meteorology, Atmospheric Science Option **Expected May 2012**
Pennsylvania State University, University Park, PA
- Schreyer Honors College
- Minor in Mathematics

PROFESSIONAL EXPERIENCE:

Undergraduate Research **March 2011- Present**
Department of Meteorology, Pennsylvania State University, University Park, PA
“GFS Forecast Skill for Long-Lived Tropical Disturbances”

NOAA Ernest F. Hollings Intern **May 2011- July 2011**
NOAA National Severe Storms Laboratory, Norman, OK
“Convective Parameters from the 20th Century Reanalysis”

Undergraduate Research **March 2010-August 2010**
Department of Meteorology, Pennsylvania State University, University Park, PA
“The Observed Response of Climate Variables to Tropical SST Anomalies”

COMPUTER SKILLS:

- Advanced NCAR Command Language (NCL)
- Intermediate Fortran
- Intermediate Matlab
- Experience running the WRF-ARW model

AWARDS:

- Dean Steidle Scholar Award, 2012
- John A. Dutton Award in Atmospheric Dynamics, 2012
- NOAA Ernest F. Hollings Scholarship, 2010-2012
- Schreyer Honors College Academic Excellence Scholarship, 2008-2012
- Quentin and Louise Wood Honor Scholars Award, 2011-2012
- Dean’s List, 2008-Present
- John and Elizabeth Holmes Teas Scholarship, 2009-2011
- Chelius Family Scholarship in Meteorology, 2008-2011
- Matthew J. Wilson Honors Scholarship, 2008-2009

PRESENTATIONS:

- “Convective Parameters from the 20th Century Reanalysis,” *AMS 11th Annual Student Conference*, New Orleans, Louisiana; 1/2012.